The Astrophysical Journal Letters, 803:L8 (5pp), 2015 April 10 doi:10.1088/2041-8205/803/1/L8
© 2015. The American Astronomical Society. All rights reserved.

SUPERNOVA REMNANT MASS ACCUMULATED DURING THE STAR FORMATION HISTORY OF THE $z = 3.8$ RADIO GALAXIES 4C41.17 AND TN J2007-1316

B. Rocca-Volmerange[1,2], G. Drouart[3], and C. De Breuck[4]
[1] Institut d'Astrophysique de Paris, UPMC/CNRS,98bis Bd Arago, F-75014 Paris, France; rocca@iap.fr
[2] Université Paris-SUD, F-91405 Orsay, France
[3] Chalmers University of Technology, Onsala Space Observatory, SE-43992 Onsala, Sweden
[4] ESO, Karl Schwarzschild Str. 2, D-85748 Garching-bei-München, Germany
Received 2014 November 28; accepted 2015 March 19; published 2015 April 8

ABSTRACT

In this paper, we show that the supernova remnant (SNR) masses accumulated from core-collapse supernovae (SNe) along the star formation history of two powerful $z = 3.8$ radio galaxies, 4C41.17 and TN J2007-1316, reach up to $\geqslant 10^9\,M_\odot$, which is comparable to supermassive black hole (SMBH) masses measured from the SDSS sample at similar redshifts. The SNR mass is measured from the already exploded SN mass after subtraction of ejecta while the mass of still luminous stars fits at best the observed spectral energy distribution, continuously extended to the optical–*Spitzer*–*Herschel*–submm domains, with the help of the galaxy evolution model Pégase.3. For recent and old stellar populations, SNR masses vary about $10^{9-10}\,M_\odot$ and the SNR–to–star mass ratio between 1% and 0.1% is comparable to the observed low-z SMBH–to–star mass ratio. For the template radio galaxy 4C41.17, SNR and stellar population masses estimated from large aperture (>4 arcsec = 30 kpc) observations are compatible, within one order of mass, with the total mass of multiple optical *Hubble Space Telescope* (700 pc) structures associated with VLA radio emissions, both at 0.1 arcsec. Probing the SNR accretion fueling central black holes is a simple explanation for SMBH growth, which requires the physics of star formation and stellar and galaxy dynamics with consequences for various processes (quenching, mergers, negative feedback) and is also a key to the bulge–SMBH relation.

Key words: galaxies: elliptical and lenticular, cD – galaxies: evolution – galaxies: high-redshift – galaxies: individual (4C41.17) – galaxies: starburst – quasars: supermassive black holes

1. INTRODUCTION

The scaling relations found up to $z = 5$ (Magorrian et al. 1998; Ferrarese & Merritt 2000) between supermassive black hole (SMBH) mass $M_{\rm SMBH}$ and properties of spheroidal hosts such as the stellar velocity dispersion σ, the V-band luminosity L, and the bulge stellar mass $M_{\rm bulge}$ have been recently confirmed at the centers of nearby galaxies (McConnell 2013). However, the origin of such a tight relationship between SMBHs and galaxy star formation history is still actively debated (Kormendy & Ho 2013). The main question is whether the huge difference in size scales between the galaxy core ($\simeq$1 pc) embedding the SMBH and the galaxy and its environment (from 10 to 100 kpc) is justified. At the core scale, the central black hole grows via fluid accretion (Blandford & Begelman 2004) and has already reached $10^{9-10}\,M_\odot$ at the highest redshifts (Vestergaard et al. 2008). From a gas point of view, because disk outflows are estimated insufficiently to justify the SMBH growth, active galactic nucleus (AGN) feedback is simultaneously proposed to explain the $M_{\rm SMBH}$–σ relation and to quench the star formation activity in early-type galaxies (Gabor & Bournaud 2014). However, even if a large number of feedback models are supported by many surveys (X-rays, radio VLA, PEP, GOODS-*Herschel*, CANDELS-*Herschel*), difficulties remain in explaining any accretion process from variable AGNs, which have never been observed to be turned on or off by star formation.

From a star point of view, detailed analyses of stellar processes near the massive black hole in the Galactic Center system (Alexander 2005; Genzel 2014) have studied the mass segregation driving stellar dense matter (neutron stars and stellar black holes) toward the central black hole through dynamical friction (Chandrasekhar 1943; Binney & Tremaine 2008). Adopting the universality of the initial mass function (IMF), the supernova remnant (SNR) mass of old stellar populations is weighted for a few percent of the total galaxy mass (Magorrian et al. 1998). However, at high redshifts, stellar population properties (mass, size, density, velocity dispersion, drag timescale) depend on cosmology and galaxy evolution: at $z = 3.8$, the look-back time is more than 80% of the cosmic time. Thus if SNRs are eternal and have time to segregate, the SNR–black-hole relation via dynamical friction depends on galaxy evolution parameters, in particular the star formation rate (SFR) by galaxy type, and evolving star populations need to be followed with an evolutionary code such as the Pégase code.

The AGN–starburst relation is often based on SFR estimates derived mostly from mid- and far-infrared (far-IR) luminosities (Kennicutt 1998). However, the SFR calibration suffers from uncertainties in the disentangling of the emissions by the AGN torus and by cold grains in the radiative transfer modeling of grain absorption/emission through various geometries and in the ultraviolet to optical contribution of young star photospheres. Moreover, a time delay of the dust emission peak is induced by the lifetime duration of supernovae (SNe), the ejecta of which are sources of interstellar metal enrichment and dust grains. As a consequence, most SFR estimates derived from the observed far-IR emissions are due to less massive populations, still luminous after the SN explosions, implying an underestimation that needs to be corrected with evolution models. Calibration of the SFR requires coherence between various tracers by taking into account stellar passive evolution with the help of evolutionary spectrophotometric and chemical

models, e.g., the Pégase.3 code (Fioc & Rocca-Volmerange 1997), recently improved with grain C and Si enrichment and radiative transfer computed by Monte-Carlo simulations (near submission).

Powerful radio galaxies are preferentially selected for their detection at the highest redshifts ($z > 5$), for their signatures of starburst and AGN activities through continuum and emission lines, and for the presence of an SMBH. From the Herge catalog (Drouart et al. 2014) of 70 $1 < z < 5.2$ radio galaxies observed with the *Herschel* and *Spitzer* satellites, completed by UV, optical, and submm observations, the two $z = 3.8$ radio galaxies 4C41.17 and TN J2007-1316 have been selected for their low AGN activity favoring a dominant stellar origin for far-IR dust emission. Their continuous spectral energy distributions (SEDs) have been fitted (Rocca-Volmerange et al. 2013) according to the usual evolutionary spectral synthesis procedure (Le Borgne & Rocca-Volmerange 2002). Fits are processed in the observer frame (and not in the rest frame) using libraries of template spectra for starbursts and Hubble Sequence galaxies, corrected for universe expansion and galaxy evolution, with various input parameters (initial metallicity and mass function IMF).

Hereafter, the new point is to estimate the SNR masses predicted by star formation histories of elliptical galaxies supposed to host distant radio galaxies, assuming the universality of the IMF. Derived from evolutionary models calibrated to observed low resolution SEDs, SNR and star masses are globally compatible with the high resolution (0.1 arcsec) *Hubble Space Telescope* (*HST*) and VLA data. Galaxy evolution models follow at any galaxy age and type (i) the already exploded SN population, (ii) the consequent metal enrichment, (iii) the SNR mass, and (iv) the mass of residual luminous stars. In Section 2, the SNR mass of a single stellar population (SSP) $M_{\rm SNR}^{\rm SSP}(t)$ and of Hubble Sequence galaxy scenarios $M_{\rm SNR}^{\rm Gal}(t)$ are derived at age t. Section 3 shows the best fits of SEDs, stellar masses, metallicities, and SNR masses for the two radio galaxies. Section 4 analyzes the high resolution images of 4C41.17 in terms of SNR and resolved stellar masses and of their compatibility with radio and optical (700 pc) structures. The last section is a discussion of model degeneracy and perspectives.

2. EVOLUTION OF ACCUMULATED MASSES OF SNRs AND STARS

2.1. Single Stellar Population

In the SSP formalism, the number of stars formed per mass and time units is at time t:

$$d^2N(m, t) = \delta(t)\ \Phi(m)\ dm\ dt,$$

where $\delta(t)$ is the instantaneous SFR(t) and $\Phi(m)$ is the IMF.

The SNR (black hole or neutron star) is produced during the terminal phase of the iron core-collapse of massive SN explosions—SN II, SN Ib, and others—followed by a shock wave rebound ejecting the envelop of enriched gas. At any age, the SN number and their corresponding ejecta from yields (Portinari et al. 1998; Marigo 2001), depending on the initial metallicity of the SSP, are followed with the help of the evolutionary code Pégase (Fioc & Rocca-Volmerange 1997; see also www2.iap.fr/pegase) in its last version Pégase.3 (near submission).

At age t of the SSP, the SNR mass $m_{\rm SNR}$ is accumulated from the successive generations of stars exploding as SNe between 0 and t:

$$M_{\rm SNR}^{\rm SSP}(t) = \int_{t'=t_{\rm PSN}^{\rm min}}^{\rm min\,(t_{\rm PSN}^{\rm max},t)} m_{\rm SNR}\left(m_{\rm PSN}(t')\right) \times\ \Phi\left(m_{\rm PSN}(t')\right)\left|\frac{dm_{\rm PSN}}{dt}\right|(t')dt'$$

where $m_{\rm SNR}\left(m_{\rm PSN}(t')\right) = (m_{\rm PSN} - m_{\rm ej})(t')$ with $m_{\rm PSN}$ being the presupernova mass, $m_{\rm ej}$ the mass fraction of metal-enriched gas ejecta, including winds during evolution, and $t_{\rm PSN}$ being its lifetime duration depending on the initial mass extended from the minimum up to the maximum progenitor lifetime durations. The Kroupa standard IMF (Kroupa 1997) is limited between the extreme values $M_{\rm sup} = 120\,M_\odot$ and $M_{\rm inf} = 0.09\,M_\odot$ with SN precursors from 120 to 8 $M_\odot$. The stellar mass $M_{\rm star}^{\rm SSP}(t)$ of the SSP at age t corresponds to masses of still luminous stars, which are less massive than past SN progenitors and passively evolving according to stellar evolution tracks. The respective evolutions of the current $M_{\rm star}^{\rm SSP}(t)$ and of $M_{\rm SNR}^{SSP}(t)$ are opposite up to $\simeq$50 Myr, the lifetime duration of the lowest mass SNe.

2.2. SNR and Star Masses Derived from Galaxy Scenarios by Type

The star formation laws by galaxy type modeled with the code Pégase.3 (Figure 1, top) are calibrated on local templates of the Hubble Sequence by fitting only three gas-regulation parameters (infall timescale, outflow age, and a gas-dependent SFR such as the Kennicutt–Schmidt law) and the choice of the IMF (see www.iap.fr/pegase.2). A comparison with the observed local SDSS data sample is presented in the color–color *g-r/r-i* diagram (Figure 1, bottom). Except for the most extreme red and blue galaxies, star formation laws give synthetic templates compatible with observations. Laws by type mainly differ by their star formation timescales from $\simeq$1 Gyr for early types up to $\simeq$10 Gyr for late spirals (Rocca-Volmerange et al. 2004). In particular, the elliptical galaxy scenario shows its maximal efficiency at $z \simeq 8$ for a formation redshift $z_{\rm for} = 10$. Because of the cosmic time–redshift relation t–z, changing $z_{\rm for}$ in the interval [5, 30, or more] will not significantly modify the scenario parameters. For each galaxy type, the SNR mass $M_{\rm SNR}^{\rm Gal}(t)$ is derived from the accumulated number of SNe, after subtraction of ejecta.

3. MASSES AND AGES OF THE $z = 3.8$ RADIO GALAXIES 4C41.17 AND TN J2007-1316

The SNR and star masses are derived from the best fits of the continuous UV to submm SEDs (Rocca-Volmerange et al. 2013), covering *Herschel, Spitzer*, VLT, and submm ground-based data. The choice of faint AGN radio galaxies allows one to disentangle the emission of stellar populations from that of the AGN torus (Figure 2, green dashed line). The χ^2 procedure is based on large libraries of SSPs and galaxy scenarios by type built at ages 0–20 Gyr, various IMFs (Kroupa and Salpeter), initial metallicities ($Z = 0$ to 0.02), and gas-and-metal column density mass/r^2 varying as 0.1, 1, 10× the local gas column density NHI.

For the two radio galaxies, the SSP model fits the optical and far-IR data (Figure 2, blue line) at the same age of 30–35 Myrs (the lifetime duration of a 9 $M_\odot$ supernova) with a Kroupa IMF

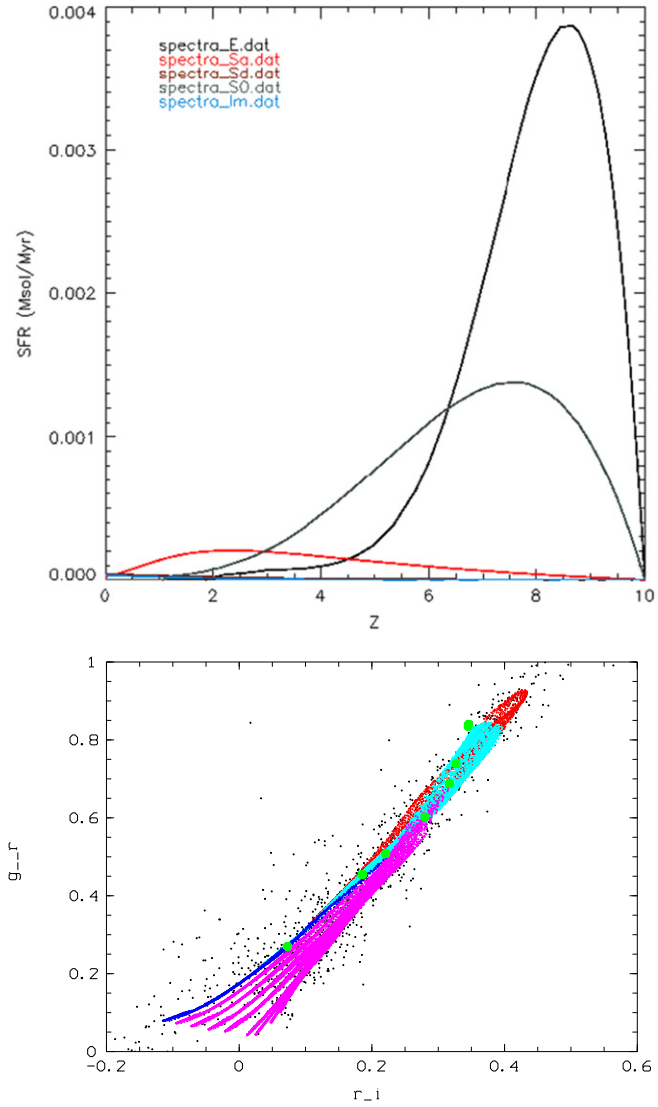

Figure 1. Top: adopted star formation laws for types Ell, S0, Sa, Sd, and Irregular (Im) galaxies as a function of z in arbitrary units (Le Borgne & Rocca-Volmerange 2002). Bottom: comparison of synthetic templates of Ell (red), S0 and Spirals (turquoise), Im (dark blue), and quenched (pink) galaxies with observed local SDSS galaxies (black points) in the color–color *g-r/r-i* diagram (Tsalmantza et al. 2012). Green points correspond to the adopted star formation laws.

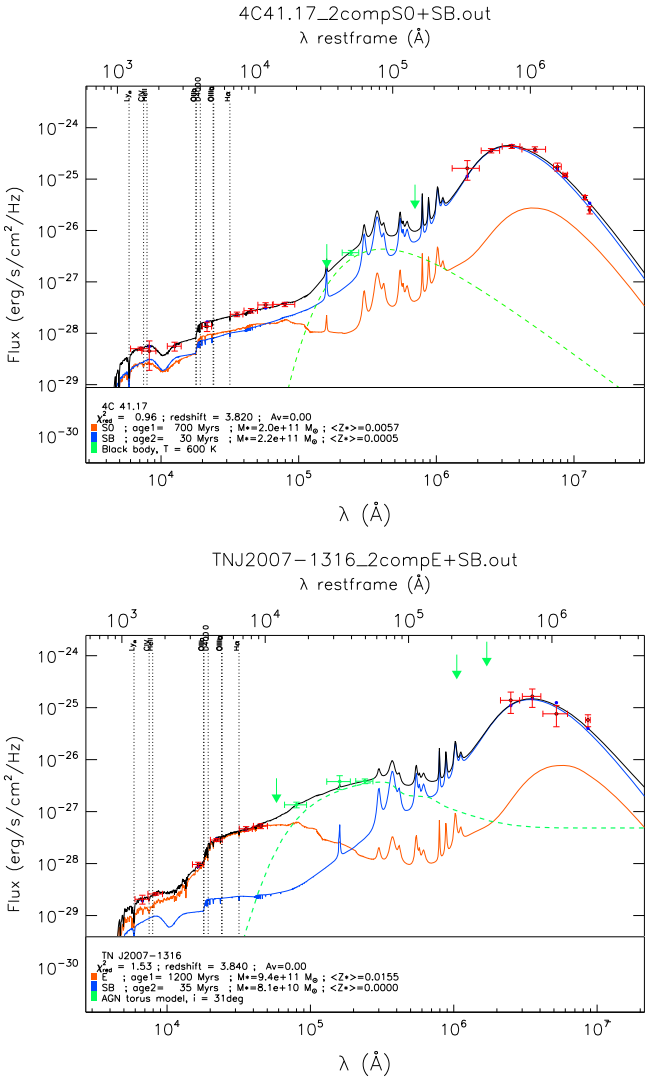

Figure 2. Observations are red crosses and global SED fits are black lines for the two galaxies. Left: 4C41.17, a young starburst (blue line) with age = 30 Myr, $M_{\rm star} = 2.2 \times 10^{11}\,M_{\odot}$, $Z = 510^{-4}$ plus an early-type old scenario (orange line) with age = 0.7 Gyr, $M_{\rm star} = 2.0 \times 10^{11}\,M_{\odot}$, $Z = 5.7 \times 10^{-3}$. Right: TN J2007-1316, a young starburst (blue line) of age = 35 Myrs, $M_{\rm star} = 0.8 \times 10^{11}\,M_{\odot}$, $Z < 10^{-4}$ and an early-type old scenario (orange line) of age = 1.2 Gyr, $M_{\rm star} = 9.4 \times 10^{11}\,M_{\odot}$, $Z = 1.55 \times 10^{-2}$. Blackbody or Pier AGN models (dashed green line) are compatible with superior limits (green arrows). Standard cosmology parameters are used ($\Omega_M = 0.3$, $\Omega_\Lambda = 0.7$, $H_0 = 72$ km s^{-1} Mpc^{-1}).

in a dense medium (10 × local value $\simeq 10^{22}\,{\rm cm}^{-2}$). The old elliptical/S0 model mainly fits the SED peak in the near-IR to *Spitzer* domain, at cosmic ages $\simeq$1 Gyr (respectively 0.7 and 1.2 Gyr) with a Kroupa IMF in a high-density medium (Figure 2, orange line). In agreement with ages and masses of luminous stars from these best fits, SNR masses are derived for the young and old past stellar populations of the two galaxies.

Table 1 provides the age, star mass $M_{\rm star}$, SNR mass $M_{\rm SNR}$, the $M_{\rm SNR}/M_{\rm star}$ ratio, and metallicity Z of the young (evolved SSP) and old (Elliptical/S0) stellar components for the two radio galaxies, both best-fitted with the respective values of the reduced $\chi^2 = 0.96$ for 4C41.17 and $\chi^2 = 1.53$ for TN J2007-1316. SNR masses vary from 3.4 to 19 × $10^9\,M_{\odot}$ with ratios $M_{\rm SNR}/M_{\rm star}$ varying from 2.1×10^{-3} to 4.2×10^{-2}. The striking result is that the SNR mass $M_{\rm SNR}$ is of a few 10^9 to $10^{10}\,M_{\odot}$, quite comparable to SMBH masses. SNR masses $M_{\rm SNR}$ increase by less than a factor of two when changing from the Kroupa IMF to the Salpeter IMF: the massive star slopes are $\Phi(m) \propto m^{-2.6}$ (Kroupa) and $\propto m^{-2.35}$ (Salpeter). Exotic IMFs, as top-heavy ones, are not considered as they are unable to predict the typical 1 μm peak of red population for evolved early-type galaxies.

The SNR masses $M_{\rm SNR}$ are quite comparable to SMBH masses $M_{\rm SMBH}$ measured at similar redshifts (Vestergaard et al. 2008) from the SDSS-DR3 15,000 quasar sample with redshifts between 0.3 and 5.0. At $z = 3.8$, the medium value is $10^{9.3}$ in excellent agreement with our estimates of SNR masses $M_{\rm SNR}$.

To summarize, the evolved luminous stellar population fitting the SED of $z = 3.8$ radio galaxies allows one to estimate a population of already exploded SNRs, the mass $M_{\rm SNR}(t)$ of which is of the order of SMBH masses $M_{\rm SMBH}$ observed at

Table 1
Age, Star Mass $M_{\rm star}$, SNR Mass $M_{\rm SNR}$, $M_{\rm SNR}/M_{\rm star}$ Ratio, and Metallicity Z of the Young (SSP) and Early-type (Elliptical/S0) Components of the Two $z = 3.8$ Radio Galaxies 4C41.17 and TN J2007-1316

Galaxy /Component	Age	Star Mass	SNR Mass	$M_{\rm SNR}/M_{\rm star}$	Z
4C41.17/ SSP	30 Myr	2.2×10^{11}	8.5×10^{9}	3.8×10^{-3}	0.0005
TN J2007-1316/ SSP	35 Myr	8.1×10^{10}	3.4×10^{9}	4.2×10^{-2}	0.0001
4C41.17/ S0	0.7 Gyr	2.0×10^{11}	4.3×10^{9}	2.1×10^{-3}	0.0057
TN J2007-1316/ Ell.	1.2 Gyr	9.4×10^{11}	1.9×10^{10}	2.0×10^{-2}	0.0155

Note. Mass unit is $M_\odot$.

similar redshifts. The same result is found for the two distant radio galaxies, both hosted by massive ellipticals.

4. SNRs AND STELLAR POPULATIONS AT LOW AND HIGH ANGULAR RESOLUTIONS

SNR masses $M_{\rm SNR}$ of $10^{9-10}\ M_\odot$, comparable to the $10^{9.3}\ M_\odot$ of SMBH masses from the SDSS-III quasar sample, also agree with galaxy masses derived from the VLT broad Hα line emission from the nucleus of distant powerful radio galaxies (Nesvadba et al. 2011). Moreover, from the best fits, the ratio $M_{\rm SNR}/M_{\rm star}$ is $\simeq 10^{-2}$ to 10^{-3} comparable to the local ratio of $M_{\rm SMBH}/M_{\rm star}$. Recently, the discovery of the Himiko galaxy (Ouchi et al. 2013) at $z \simeq 7$, with low dust and metal content, has revealed the preliminary phase of intense star formation through UV light and the CII line, prior to SN explosions and to dust attenuation from their ejecta enrichment. The current SFR of the evolved component of the two radio galaxies is respectively 243 and 77 $M_\odot\ {\rm yr}^{-1}$ giving an SFR surface density of a few hundred $M_\odot\ {\rm yr}^{-1}\ {\rm kpc}^{-2}$ if the stars are distributed over a radius of about 750 pc around the center at an age of $\simeq$1 Gyr (Walter et al. 2009).

Our results depend on the adopted evolution scenario of early-type galaxies which is robust. Forming the bulk of stars within a 1 Gyr timescale, this scenario predicts the reddest colors of ellipticals in the $z = 0$ color–color diagram, traces the sharp limit of the $z = 0$ to 4 K-z Hubble diagram with an evolution of $10^{12}\ M_\odot$ radio galaxy hosts (Rocca-Volmerange et al. 2004) in Figure 4, reproduces photometric redshifts comparable to spectroscopic ones up to $z = 4$, and justifies the faintest multi-wavelength deep galaxy counts (Fioc & Rocca-Volmerange 1999; Le Borgne & Rocca-Volmerange 2002).

Another factor is the angular resolution of 7.23 kpc arcsec^{-1} at $z = 3.8$ with a cosmology of $\Omega_\Lambda = 0.73$, $\Omega_m = 0.27$ and $H_0 = 71\ {\rm km\ s^{-1}\ Mpc^{-1}}$. At low spatial resolution and for the two radio galaxies, SNR masses are derived from the continuous optical–IR–submm SEDs rebuilt at the aperture $\simeq$4 arcsec (Rocca-Volmerange et al. 2013). At higher resolution, the template radio galaxy 4C41.17 was observed with *HST* in the optical (Miley et al. 1992) and with VLA on a multifrequency radio continuum, in particular at 8.3 GHz (Carilli et al. 1994). At the same 0.1 arcsec resolution, multiple structures of $\simeq$500 pc size are identified. The remarkable similarity between the optical and radio morphologies of these structures is confirmed: the evolved stellar components such as H1 to H4 are within the error bars, located on compact radio emission zones B1–B2–B3 with the core N between B1 and B2; see Figure 1(c) and plate 55 of (Carilli et al. 1994). The similarity of the individual structures implicitely links evolved stars and radio jets. More recently, near-infrared integral field spectroscopy with Gemini ALTAIR NIFS (Steinbring 2014) at a similar resolution of 0.1 arcsec confirms the clumpy evolved structures and identifies a bow shock, possibly tracing recent star formation. Interpreted as active nuclei of galaxies from their flat radio emissions, the 0.1 arcsec resolved images witness evolved stars and black holes emitting radio jets, possibly fueled by SNRs. The rough approximation of a compact black hole population from a rapid starburst episode of 10^6 yr due to jet-triggered shocks (Bicknell et al. 2000; Steinbring 2014) spiraling toward the center of the galaxy through the stellar structure supposed a singular isothermal sphere (Binney & Tremaine 2008) loosing its angular momentum via dynamical friction to the galaxy core gives the following timescale:

$$t_{\rm fric,clump} = \frac{19\ {\rm Gyr}}{\ln \Lambda}\left(\frac{r_i}{5\ {\rm kpc}}\right)^2 \frac{\sigma}{200\ {\rm km\ s^{-1}}} \times \frac{10^8\, M_\odot}{M_{\rm SNR}} = 9.510^{-2}\ {\rm Gyr}$$

for $r_i = 0.25$ kpc, $M_{\rm SNR} = 2 \times 10^7\, M_\odot$ of an individual structure with $M_{\rm SNR}/M_{\rm star} = 2 \times 10^{-3}$, and $M_{\rm star} = 10^{10}\, M_\odot$ with the highest observed value $\sigma = 400\ {\rm km\ s^{-1}}$ (McConnell 2013) and a low impact parameter Coulomb logarithm $\ln \Lambda = \ln\left(b_{\rm max}/b90\right) = 5$. This average value of $\simeq$0.01 Gyr respects the Hubble time. However, more refined computations are required because the mass and the number of stellar black holes are depending on the starburst age and IMF. Moreover, the stellar dense matter is not a compact black hole.

The high resolution observations confirm that the 500–700 pc structures witness an intermediate phase of evolution before the build up of exponential disks, dense bulges, and SMBHs. At $z = 3.8$, the evolution timescale of $\simeq$1 Gyr is too short to follow the timescale of secular evolution to be completed by numerical models (Noguchi 1999; Elmegreen et al. 2008), respecting the $z = 3.8$ constraints. The SINFONI/VLT data on $z \simeq 2$ star-forming galaxies (Genel et al. 2008; Genzel 2014) suggest a scenario predicting the fraction of the central bulge mass increasing secularly over timescales of less then a few Gyr, even without major mergers. Recent observations of dense cores in massives galaxies (van Dokkum et al. 2014) out to $z = 2.5$ are also compatible with these early-type evolution scenarios.

5. DISCUSSION

The *Herschel* far-IR emission is not as direct a tracer of SFR as are ionized gas emission lines or the UV light continuum: a time delay is required to enrich the ISM in O, C, and Si through SN ejecta and to produce the dust grain mass required to fit *Herschel* data. Typically, the maximum far-IR emission peaks at age $\simeq$1 Gyr in the elliptical scenario.

After such a time delay, SN explosions created a population of dense matter remnants (stellar black holes and neutron stars), the number and mass of which depend on star formation history (rate and IMF) and galaxy age while the still alive luminous stellar population following stellar evolution principles is measurable through the multi-wavelength galaxy SED.

The accuracy of SNR and bulge masses depends on the quality of the χ^2 minimization procedure fitting SEDs, mainly constrained by the far-IR/submm luminosity coherent with the UV–optical attenuation factor while the mid-IR may reveal the old giant star population at $z = 3.8$ (see Figure 2 (bottom): the 1micron peak of the red sequence in the TN J2000-1316 SED). The degeneracy of modeling, higher (60%) for the old population than for the young one's (20%) is, however, limited because the optical domain is strongly contrained by the attenuation from metals regulating the dust far-IR emission. The far-IR is essential but not sufficient for the young component and remains less constraining for the old components. The AGN model and the far-UV polarization (3%), which could contribute to the degeneracy, are hardly concerned in the analysis of these two radio galaxies (see G. Drouart et al., in preparation).

Finally, owing to the high spatial resolution, individual stellar structures associated with radio jets are identified during an intermediate phase of galaxy evolution. In each structure, the bulk of evolved stars has already formed from intense SFR within $\simeq$1 Gyr. The further phase, not yet seen at $z = 3.8$, will be the formation of dense massive bulges and SMBH followed by detailed numerical simulations of bulge formation in galaxies (Elmegreen et al. 2008; Sales et al. 2012; Dubois et al. 2014) or in clusters (Antonini 2014), all respecting this intermediate phase of evolution.

To summarize, if the SNR population is demonstrated to migrate toward the nucleus fueling the central black hole and to be a possible source of radio jets, the dense matter is only formed from stars. There is no more need for extra formation of dark matter by black hole mergers, quenching star formation, or negative AGN feedback; all are complex processes not significantly confirmed by observations.

Statistical results from SMBH mass functions compared to stellar mass functions at high redshift, in particular from large surveys as EUCLID will confirm the keys of the AGN–star-formation relations. Moreover, the transfer of SNRs and the inspiraling process of such a huge number of stellar black holes contributing to the SMBH growth as possible cases of coalescence of two nuclear galaxy black holes will be among the most important class of gravitational wave sources for the future space-based interferometer *eLISA* (Amaro-Seoane et al. 2012).

We thank the referee for helpful remarks that have improved the manuscript. We also thank Michel Fioc for many developments in the code Pegase.3 and Jean-Philippe Beaulieu for his well-advised comments. This work is based on observations made with the *Herschel Telescope*, an ESA space observatory with science instruments provided by European-led Principal Investigator consortia and with important participation from NASA and with the *Spitzer Space Telescope* which is operated by the Jet Propulsion Laboratory, California Institute of Technology under a contract with NASA.

REFERENCES

Alexander, T. 2005, arXiv:astro-ph/0508106
Amaro-Seoane, P., Aoudia, S., Babak, S., et al. 2012, CQGra, 29, 124016
Antonini, F. 2014, ApJ, 794, 106
Blandford, R. D., & Begelman, M. C. 2004, MNRAS, 349, 68
Bicknell, G. V., Sutherland, R. S., van Breugel, W. J. M., et al. 2000, ApJ, 540, 678
Binney, J., & Tremaine, S. 2008, Galactic Dynamics (2nd ed.; Princeton, NJ: Princeton Univ. Press)
Carilli, C. L., Owen, F. N., & Harris, D. E. 1994, AJ, 107, 480
Chandrasekhar, S. 1943, ApJ, 97, 255
Drouart, G., De Breuck, C., Vernet, J., et al. 2014, A&A, 566, 53
Dubois, Y., Volonteri, M., Silk, J., Devriendt, J., & Slyz, A. 2014, MNRAS, 440, 2333
Elmegreen, B., Bournaud, F., & Elmegreen, D. 2008, ApJ, 684, 829
Ferrarese, L., & Merritt, D. 2000, ApJL, 539, L9
Fioc, M., & Rocca-Volmerange, B. 1997, A&A, 326, 950
Fioc, M., & Rocca-Volmerange, B. 1999, A&A, 344, 393
Gabor, J. M., & Bournaud, F. 2014, MNRAS, 441, 1615
Genel, S., Genzel, R., Bouché, N., et al. 2008, ApJ, 688, 789
Genzel, R. 2014, arXiv:astro-ph/1410.8717v1
Kennicutt, R. C. 1998, ARA&A, 36, 189
Kormendy, J., & Ho, L. C. 2013, ARA&A, 51, 511
Kroupa 1997, arXive:astro-ph/9705133
Le Borgne, D., & Rocca-Volmerange, B. 2002, A&A, 386, 446
Magorrian, J., Tremaine, S., Richstone, D., et al. 1998, AJ, 115, 2285
Marigo, P. 2001, A&A, 370, 194
McConnell, N. 2013, Ma, Chung-P ApJ, 764, 184
Miley, G. K., Chambers, K. C., van Breugel, W. J. M., & Macchetto, F. 1992, ApJL, 401, L09
Nesvadba, N., De Breuck, C., Lehnert, M. D., et al. 2011, A&A, 525, 43
Noguchi, M. 1999, ApJ, 514, 77
Ouchi, M., Ellis, R., Ono, Y., et al. 2013, ApJ, 778, 102O
Portinari, L., Chiosi, C., & Bressan, A. 1998, A&A, 334, 505
Rocca-Volmerange, B., Drouart, G., De Breuck, C., et al. 2013, MNRAS, 429, 2780
Rocca-Volmerange, B., Le Borgne, D., De Breuck, C., Fioc, M., & Moy, E. 2004, A&A, 415, 931
Sales, L., Navarro, J., Theuns, T., et al. 2012, MNRAS, 423, 1544
Steinbring, E. 2014, AJ, 148, 10
Tsalmantza, P., Karampelas, A., Kontizas, M., et al. 2012, A&A, 537, 42
van Dokkum, P., Bezanson, R., van der Wel, A., et al. 2014, ApJ, 791, 45
Vestergaard, M., Fan, X., Tremonti, C., Osmer, P., & Richards, G. 2008, ApJL, 674, L1
Walter, F., Riechers, D., Cox, P., et al. 2009, Natur, 457, 699